



1

2

3

4 **Are precipitation anomalies associated with aerosol variations over** 5 **Eastern China?**

6 Xiangde Xu¹, Xueliang Guo^{1,2,*}, Tianliang Zhao^{3,*}, Xingqin An¹, Yang Zhao¹, Jiannong Quan⁴, Fei
7 Mao¹, Yang Gao⁴, Xinghong Cheng¹, Wenhui Zhu¹, and Yinjun Wang¹

8 ¹State Key Laboratory of Severe Weather (LASW), Chinese Academy of Meteorological Sciences, Beijing 100081, China,

9 ²Key Laboratory for Cloud Physics, Chinese Academy of Meteorological Sciences, Beijing 100081, China, ³Collaborative

10 ³Innovation Center on Forecast and Evaluation of Meteorological Disasters, Key Laboratory for Aerosol-Cloud-Precipitation
11 of China Meteorological Administration, Nanjing University of Information Science & Technology, Nanjing 210044, China,

12 ⁴Beijing Weather Modification Office, Beijing 100089, China

13 * *Correspondence to:* Tianliang Zhao (lzhao@nuist.edu.cn)

14 **Abstracts.** In Eastern China (EC), strong anthropogenic emissions deteriorate the atmospheric environment harbored by the
15 upstream Tibetan and Loess Plateaus, building a south-north zonal distribution of high anthropogenic aerosols. This research
16 analyzed the interannual variability of precipitations with different intensities in the EC region from 1961 to 2010. We found
17 that the frequency of light rain significantly decreased and the occurrence of rainstorm, especially the extraordinary
18 rainstorm significantly increased over the recent decades. The extreme precipitation events presented the same interannual
19 variability pattern with the frequent haze events. Moreover, the extreme rainfall events of various intensities showed a
20 regular interannual variability trend. During the 1980s, the regional precipitation trends in EC showed an obvious
21 “transform” from more light rain to more extreme rainstorms. The running correlation analysis of interdecadal variation
22 further verified that the correlation between the increasing aerosol emissions and the frequency of abnormal precipitation
23 events tended to be more significant in the EC. The correlation between atmospheric visibility and low cloud amounts, which
24 are both closely related with aerosol concentrations, had a spatial distribution of “northern positive and southern negative”
25 pattern, and the spatial distribution of the frequency variability of regional rainstorms was “southern positive and northern
26 negative”. After the 1990s, the visibility in summer season deteriorated more remarkably than other seasons, and the light
27 rain frequency decreased obviously while the rainstorm and extraordinary heavy rainfall occurred more frequently. There
28 were significant differences in the interdecadal variation trends in light rain and rainstorm events between the high aerosol
29 concentration areas in the EC and the relatively “clean area” in western China. The aircraft measurements over the EC
30 confirmed that the diameters of cloud droplets decreased under high aerosol concentration condition, thereby inhibiting weak
31 precipitation process.



32 1. Introduction

33 It is widely acknowledged that the global mean temperature has been increasing since 1850 and will continue to increase in
34 the following decades (IPCC, 2007). The long-term forcing of a warming environment might change precipitation, the
35 regional and global water cycle (Allan and Soden, 2008; Allan and Ingram, 2002). The heavy precipitation events showed a
36 overall increasing trend as the result of global warming (Allan and Ingram, 2002; Trenberth et al., 2003). Since the 1950s,
37 the precipitation has increased remarkably at high latitudes, also increased at tropical marine areas, but it underwent some
38 decrease at tropical mainland (New et al., 2001; Kumar et al., 2006; Bosilvoich et al., 2005).

39 The variation of aerosols in atmosphere is also an important factor to influence the water cycle in regions where bearing
40 long-term high aerosol loading (Ramanathan et al., 2005; Ramanathan et al., 2007; Koren et al., 2008; Levin and Cotton,
41 2009; Li et al., 2011). Under the background of global warming, the regional precipitation tends to have more complex
42 temporal and spatial distribution patterns. The variations of precipitation could be reflected by the different-grade
43 precipitation, and even by frequency changes of extreme precipitation events (Lau and Wu, 2007), which could threaten the
44 social economy and is seriously concerned by governments, public and scientific community.

45 Precipitation is not only influenced by atmospheric circulation structure related with land-sea discrepancy and land-sea water
46 vapor exchange, but also by local cloud microphysical processes (e.g., CCN, IN). Studies have shown that atmospheric
47 aerosols might add cloud droplets number concentrations (CDNC), and change cloud lifetime, and restrain or enhance
48 precipitation (Khain et al., 2005; Rosenfeld et al., 2007; Rosenfeld and Coauthors, 2008; Stevens and Feingold, 2009; Fan et
49 al., 2013).

50 Since the middle 1980s, China experienced a rapid development in industry and agriculture. As a result, a huge amount of
51 industrial emissions and biomass burning significantly released particulate matters into the atmosphere. The study shows that
52 there was no obvious change in annual precipitation in China, but the extremely heavy rainfall area, mainly in the EC, had
53 expanded (Zhai et al., 1999). However, the regional annual precipitation, summer precipitation, and extreme precipitation
54 events had an obvious rising tendencies in middle and lower Yangtz River Basin of EC (Wang and Zhou, 2005). The
55 numerical simulations also presented that the increase of aerosols could decrease the summer convective precipitation in the
56 intensity under 30 mm h^{-1} , and increase summer strong convective precipitation in the rates above 30 mm h^{-1} in China (Guo
57 et al., 2014). With a rapid increase of aerosols, not only local light rain over wide areas could decrease, but also local
58 extremely heavy rain could be triggered, inducing frequent flood (Guo et al., 2014; Fan et al., 2015). Light rain tended to
59 decrease and at the same time the extremely heavy precipitation had increasing tendency in the EC (Choi et al., 2008; Qian
60 et al., 2007; Qian et al., 2009). This phenomena might be the strong signal of climate variability connecting to global
61 warming together with the increased emissions of anthropogenic aerosols.

62 Aerosols might also change Asian monsoon system (Bollasina et al., 2011). There are great uncertainties in the interactions



63 between the internal influence factors including complex influences of land-sea discrepancy, aerosols and cloud and
64 precipitation processes of Asia monsoon system and external forcing factors.

65 The large amounts of anthropogenic aerosols not only deteriorate the environment over large spatial scales, but they might
66 induce the rapid change of regional climate and water cycle. In addition, the high aerosol concentration zone in the
67 north-south direction over China is located on the eastern side of the Tibetan plateau and the Loess plateau, which might be
68 connected with the leeward slopes of the large terrain structure of the plateaus. The regions from the plateaus to EC may be
69 an ideal place to identify the climate forcing of aerosols with following questions: comparing the interannual variation
70 trends in various precipitation intensities between the polluted EC with the clean region over the Tibetan plateau. The
71 previous investigations of this issue primarily focused on limited cases. The climatic forcing of aerosols on precipitation
72 extremes in large-scale continent region and its physical causes remain uncertain. By using precipitation and visibility data in
73 a 50-year period and satellite, aircraft and surface aerosol observational data in recent years in China, the climatic impacts of
74 aerosols on interannual variability of various precipitation intensities and their physical links were investigated in this study.

75 2. Data

76 In this work, we adopted annual average AOD data in 2001-2010 from Moderate Resolution Imaging Spectroradiometer
77 (MODIS); monthly frequency of different-intensity of precipitation events including extraordinary storm (>200mm, the
78 precipitation intensity classification standard for 24 hours), rainstorm (100-200mm), large rainstorm heavy rain (25-50 mm),
79 moderate rain (10-25mm), light rain (0.1-10mm) from 601 stations in China over 1961-2010 (Datasets from the National
80 Meteorological Information Center of China Meteorological Administration); In addition, the meteorological and
81 environmental data including monthly haze days of 2513 stations, daily visibility of 598 stations and daily low cloud cover
82 of 753 stations in China as well as the daily PM_{2.5} data of 946 stations in 2013-2014 in China were also used.

83 In order to analyze the regional variations in aerosols over Eastern China, we adopt the equivalent visibility by excluding the
84 influence of natural factors (Rosenfeld et al., 2007) on the observed visibility based on the meteorological data observed
85 from 598 stations in 1961-2010 were used in this study. The equivalent visibility was corrected based on the the
86 following formula (1) under the relative humidity from 40% to 99%.

$$87 \quad \frac{VIS}{VIS(dry)} = 0.26 + 0.4285 \log(100 - RH) \quad (1)$$

88 The characteristics of aerosol and cloud droplets size were comprehensively analyzed based on the aerosol-cloud data
89 obtained from aircraft flights carried out in Beijing and its surrounding regions during 2008-2010 by the Beijing Weather
90 Modification Office. The scientific detection time was from May to August during 2008-2010. The observed clouds were
91 mainly stratus cloud, stratocumulus and cumulus clouds, and the maximum detection altitude was 7000 m. There were 40
92 flights carried out during the experiment period. Aircraft measurements were usually carried out within 2-6 h before the



93 clouds precipitated. The flight area and tracks were shown in Fig. 1. The Passive Cavity Aerosol Spectrometer Probe
94 (PCASP-200, DMT Co.) was used for observing aerosol particle size in 0.1-0.3 μm . The probe of Cloud, Aerosol and
95 Precipitation Spectrometer (CAPS, DMT Co.) was used for observing cloud droplets in 0.6-50 μm . The probes were returned
96 to the DMT for standard calibration before starting measurements in each year. In addition, the probes were calibrated using
97 the spheres of polystyrene latex (PSL) of Duke Scientific Corporation for each month. Considering the influence of cloud
98 droplets on aerosol probing, the averaged aerosol concentration below 300m of cloud base was calculated to represent
99 aerosol concentration in clouds. The cloud droplet measurements were made within clouds at 100m height intervals. The
100 data were processed into two or more samples when the clouds were multiply layered.

101 **3 Haze distributions in Eastern China harbored by large plateaus**

102 Due to the influence of the terrain on the typical westerly winds in Eastern China, the air flowing from the windward
103 plateaus descends in a north-south oriented zone between about 110°E and 125°E (upper panel of Fig. 2). Accompanying this
104 strong downward current are weak winds in the near-surface layers in the lee side of the plateaus. These air flow and wind
105 condition lead to development of a “harbor” accumulating air pollutants in EC. The weak wind and downward current areas
106 coincide well with the centers of frequent haze events in China (lower panel of Fig. 2). The “susceptible region” of haze
107 events over Eastern China from the eastern edge of the plateaus to the lower flatlands is associated with the “harbor” effect
108 of the unique topography under specific meteorological conditions that trap air pollutants (Xu et al., 2016).

109 **4. Change trends in various precipitation intensities**

110 The interannual variation trends of extreme precipitation events with various intensities including light rain, moderate rain,
111 heavy rain, rainstorm, the large rainstorm, extraordinary rainstorm (Fig. 3a) were comparatively analyzed and it is found that
112 the interannual variation trend differences for the six various precipitation intensities were significant. The light rain
113 frequency trend significantly decreased (Fig. 3a, A), the moderate rain frequency trend slightly declined (Fig. 3a, B), the
114 interannual change trend of heavy rain frequency was not significant (Fig. 3a, C), the rainstorm and large rainstorm events
115 increased significantly (Fig. 3a, D, E, F) in EC. Especially since 1980s, the extremely heavy precipitation events have
116 become more frequent, showing an obvious transforming characteristics of frequent heavy rain and torrential rain. Large
117 rainstorm and especially large rainstorm extreme events presented significantly an increased trend, along with the frequent
118 haze weather in EC. Overall rainstorm extreme events were on the rise trend, but light rain tended to decline significantly.
119 In contrast, stations in the Tibetan Plateau (at height of >4000m), a relative clean area in China, were selected for a
120 statistical analysis of interannual variation trend of light rain frequency, indicating that the characteristic of the decreased
121 trend of light rain frequency was not significant in the Tibetan Plateau (Fig. 3b,A).



122 5. Distribution of frequency of extreme rainstorm events and visibility

123 The negative variability area of light rain frequency almost matched with positive variability of visibility and haze frequency
124 in EC (Fig. 4a,b and c), which are well consistent with the area of high aerosol concentrations and frequent haze events (Fig.
125 2a,b). The light rain frequency reduction in China was closely associated with the enhancement of aerosol levels in the
126 atmosphere (Qian et al., 2009).

127 It is noteworthy that the negative trend areas of light rain almost covered a large part of areas in China and all eastern China
128 (Fig. 4c). This might be closely related with temporal and spatial variation trends of summer monsoon activity which offered
129 a suitable dynamic background for the effect of aerosols on clouds and precipitation. Figure 5a shows that the spatial
130 distribution of the rainstorm frequency variability was “southern positive and northern negative” in summer during
131 1961-2010, while the correlations between visibility and low-level cloud amount were distributed with the “northern positive
132 and southern negative” pattern during 1961-2010 in EC (Fig. 5b), indicating that the effect of aerosols on summer
133 convective precipitation was more obvious in southern part than that in northern part of EC.

134
135 There were obvious differences in the interdecadal precipitation decreasing rate of the various precipitation intensities in the
136 EC region (Fig. 6a). In this region, the summer interdecadal precipitation variability revealed the influence features of
137 aerosols on clouds and precipitation process, that negative variability stations of light rain made up the majority (about
138 87.6%), the positive variability stations of moderate rain were approximately equal to the negative ones (about 51%), the
139 positive variability stations of heavy rain (about 71.3%) were much more than the negative ones indicating the reverse trend.
140 The positive variability stations of rainstorm with daily precipitation >50mm, including catastrophic rainstorm over
141 100mm occupied obvious majority (about 78.9%). In China, in the recent decades, the rapid increase of the anthropogenic
142 aerosol particles in the atmosphere may make the cloud droplet number concentration increased but the size of cloud droplet
143 decreased, thus changing the life time of the cloud and suppressing the precipitation, especially for the light rain (Qian et al.,
144 2009).

145 As mentioned above, the light rain frequency reduced significantly; the moderate rain frequency changed unobvious; heavy
146 rain increased relatively obvious, rainstorm and catastrophic rainstorm increased significantly obvious in eastern China,
147 indicating the obvious change characteristics of regional precipitation from light rain changed to heavy rain and even the
148 catastrophic rainstorm along with the frequent haze trend in EC.

149 Although severe precipitation event mainly depended on dynamical and thermodynamic processes and water vapor source in
150 the atmospheric circulation and deep convective activity, aerosol's “Albrecht effect” considered that increased cloud droplet
151 concentration and decreased cloud droplet size influenced by aerosol would suppress cloud precipitation process and extend
152 cloud maintenance time. The extension of the cloud life time might save the potential that triggering the abnormal severe
153 precipitation extreme events when the cloud droplets coagulation condition was mature. This mechanism could partly



154 explain the significant light rain reduction trend (Fig. 6a) and the spatial consistency indicating the precipitation rate
155 transformation characteristics of light rain to heavy rain or severe precipitation extreme events (blue arrows in Fig. 6a) in
156 eastern China. Moreover, in this research, in order to further comparatively analyze the effects of frequent haze weather in
157 eastern China on extreme precipitation events, we selected the Tibetan Plateau (west of 110 °E, south of 40 °N), a relative
158 clean area in western China, as the reference area, and calculated frequency variability trends of light rain and rainstorm in
159 the three different interdecadal periods (1961-1980, 1971-2000, 1981-2010) in the east and west regions. As could be seen
160 from Fig. 6b (left), in the three stages, the positive variability of light rain was a declining trend while the negative variability
161 was an increasing trend in EC, while there were no obvious positive or negative variability trend of light rain and rainstorm
162 in Tibetan Plateau (double-headed arrows in Fig. 6b right).

163 **6. interannual variability between atmospheric visibility and precipitation anomalies**

164 We calculated the correlation coefficients between regional averages of visibility with the frequency of light rain, heavy rain,
165 extremely torrential rain over EC region (east to 110 °E, south to 40 °N), respectively in consideration of correlation pattern
166 between visibility and various precipitation intensities. Therefore, taking summer months (June, July and August) as
167 examples, the 20-year running correlation coefficients of visibility and precipitation were obtained (Figs. 7 a, b and c). The
168 running correlation coefficients curve of visibility and light rain reached the confidence level (90%), and the running
169 correlation coefficients curve of visibility and heavy rain and extremely heavy rain reached the confidence level (90%). This
170 statistical analysis results further verified that with the increase of aerosol emissions, visibility and various precipitation
171 exhibited increasing significant correlation trends (Fig.6).

172

173 In order to investigate the seasonal and annual correlation pattern between regional visibility and light rain, as well as
174 regional visibility and extremely precipitation events in EC, we illustrated the annual cross-section of monthly anomaly of
175 visibility and light rain, visibility and heavy rain, as well as visibility and extremely heavy rain. Through comprehensive
176 comparison of Figs. 8 a, b, c and d, we could find significant positive correlation between visibility and light rain, showing
177 that the poor visibility suppressed light rain frequency. Moreover, there was significant difference between the changing
178 trend of extremely precipitation events frequency and light precipitation frequency. The change of heavy precipitation
179 frequency from 1960s to 1980s was not as prominent as that at the latter period of 1990s, during which time visibility
180 deteriorated remarkably, heavy and extremely heavy rain occurred frequently. Compared to other seasons, the influence
181 effect of poor summer visibility was more significant in China, showing light rain frequency decreasing significantly and
182 sudden heavy rain and large heavy rain frequency increasing.

183 The increased atmospheric aerosol concentration may reduce the solar radiation to surface and decrease surface temperature.



184 At the same time, the polluted black carbon aerosols can strongly absorb solar short-wave radiation and directly heat
185 low-level atmosphere, and form a temperature inversion structure (Bollasina et al, 2011; Zhang et al., 2009; Bond et al.,
186 2013; Bond et al., 2011; Grant et al., 2014; Seinfeld et al., 2008). Therefore, the aerosol-radiation interaction could change
187 the atmospheric stability and alter local or region atmospheric circulation and precipitation process. This temperature
188 inversion structure increases the stability of atmospheric boundary layer and provides an important condition for the frequent
189 occurrence of haze and fog events. The stable low-level structure also inhibits the weak convection development of
190 atmospheric boundary layer, so as to reduce the formation of low-level clouds and weak precipitation process. However, the
191 strong dynamic convergence disturbance could destroy the stability of atmospheric boundary layer and cause the formation
192 and development of severe rainstorms.

193 To further clarify the relation between aerosol concentration and light rain frequency, the light rain frequency distribution
194 from 601 stations in July, 2013 is displayed (Fig.9). It shows in Fig. 9 that the light rain events have significantly declined in
195 the Yangtze River region of EC with high aerosol concentrations have and but enhanced while t in the relative clean region of
196 Tibetan Plateau.

197 To reveal the relationship between aerosols and atmospheric vertical thermal structure, the correlation between PM_{2.5}
198 concentration and atmospheric thermal structure in both polluted and clean areas in July, 2013 was investigated (Fig. 10).
199 The stations of Changsha and Hongjia located in Hunan and Zhejiang provinces in EC respectively were selected to
200 represent the less light rain region while those of Linzhi and Dingri of Tibet were selected to represent the high-frequency
201 light rain region. The correlation coefficient profiles between the observed surface daily PM_{2.5} concentration and
202 atmospheric temperature profiles derived from high-resolution L-band sounding were calculated. The correlations at
203 Changsha and Hongjia stations (Figs.10a-b) show that the correlation between PM_{2.5} and temperature profiles presented an
204 "inverse phase" characteristic, indicating they were negatively correlated at low boundary layer and positively correlated at
205 upper boundary layer or troposphere, reflecting the high aerosol concentrations in a thermal structure similar to temperature
206 inversion layers like "cold at low-layer and warm at upper-layer" in the eastern China. On the contrary, the correlations in
207 Linzhi and Dingri stations in the Tibetan Plateau (Fig. 9c,d) indicate that an unstable atmospheric structure with "warm at
208 low-layer and cold at upper-layer" for a favorable condition for the occurrence and development of weak convection and
209 light rain events in the Tibetan region.

210 **7. Physical connection between aerosols and precipitation**

211 According to the results of observation and modeling studies, the increased aerosol concentrations could reduced effective
212 particle radius and increased number concentration of cloud droplets, and latent heat release (Khain et al., 2005; Van den
213 Heever et al., 2006; Tao et al., 2007; Altaratz et al., 2014).The increase of cloud droplets concentrations would delay



214 raindrop formation, thereby lessening light precipitation (Qian et al., 2009) leading the negative correlation between aerosol
215 and precipitation in China (Choi et al., 2008).

216 In order to further investigate the relationship between aerosols and cloud droplets, the observed data collected by aircraft in
217 north China during 2008-2010 were used. The vertical profiles of cloud droplets data at each level under different aerosol
218 state obtained by 40 aircraft is shown in Fig. 11a. From Fig. 11a and Fig. 11b, aerosol Albrecht "cloud lifetime effect" was
219 significant in the Northern EC. As shown in red profile of Fig. 11b, under the background of high aerosol concentration, the
220 cloud droplets sizes were smaller and increased slowly with the increasing altitude. In addition, from the cloud base to
221 2000m, the cloud droplets size remained less than 20 microns (Fig.11b), resulting in precipitation delay, in favour of cloud
222 system development to form heavy rain easily. In addition, cloud droplets diameter enlarged quickly with the increase of
223 height, and reached 30 microns easily to forming light rain at 1000m altitude under low aerosol concentration (green profile
224 in Fig.11b). The above aircraft observation analysis showed that under the condition of insufficient water vapor in the North
225 China relative to that in the southern China, high aerosol concentration could reduce cloud droplets size, increase cloud
226 droplets concentration, extend cloud lifetime, and this would restrain the development of low clouds, especially restrict the
227 light rain process.

228 8. Discussion and conclusions

229 Aerosols have complicated effects on clouds and precipitation, depending on many factors such as aerosol properties,
230 topography and meteorological conditions. The most previous investigations of aerosol impacts on clouds and precipitation
231 are primarily based on limited cases in relatively smaller spatial and temporal scales. The climate forcing of aerosols on
232 precipitation in large-scale continent region and physical causes remain uncertain. By using precipitation and visibility data
233 in 50 years and satellite, aircraft and surface aerosol data in recent years in China, the impacts of aerosol variations on
234 interannual variability of various precipitation intensities of precipitation events and their physical causes are investigated.

235 Accompanied with the frequent haze events in EC, the light rain frequency trend significantly decreased. Especially, since
236 the 1980s the extremely heavy precipitation event have occurred more frequent with an obvious transform from light rain to
237 frequent heavy rain and rainstorm. From 1960s to 1970s, the monthly visibility and light rain presented a significantly
238 positive correlation, while the visibility was in good condition, and the light rain frequency was also in high value. In recent
239 20 years, the dramatically increased aerosols resulted in poor visibility, and the light rain frequency decreased obviously, and,
240 heavy and extremely heavy rain occurred more frequently.

241 The investigation of relation between aerosol concentrations and light rain frequency distributions from 601 stations in July,
242 2013 in China shows that that the light rain in the Yangtze River region of EC with high aerosol concentration appeared
243 significantly low-frequency while that in the relative clean region of Tibetan plateau presented significantly high-frequency.



244 The physical cause of this relation was investigated, and found that the high aerosol concentration was strongly correlated to
245 the low-level atmospheric warming which tended to form a stable structure that suppressed the occurrence and development
246 of weak convection and light rain events in eastern China, while this was not found in the relatively clean region over the
247 Tibetan plateau.

248 The findings from this study have some important implications: the frequent haze events in EC not only cause regional
249 environment deterioration, but also threaten the social economy and people life in large spatial and temporal scales, and
250 possible induce the long-term change of regional water cycle. This may exacerbate the effect of climate change.

251

252 **Acknowledgements**

253 The study was supported by the National Key R & D Program Pilot Projects of China (JFY2016ZY01002213;
254 2016YFC0203304), the National Natural Science Foundation of China (91544109; 91644223), the project of Environmental
255 Protection (HY14093355; 201509001) in the Public Interest and Chinese Third Tibetan Plateau Atmospheric Experiment
256 (GYHY201406001).

257 **Reference**

258 Allan, R. P. and Soden, B. J.: Atmospheric warming and the amplification of precipitation extremes, *Science* 321, 1481-1484,
259 2008.

260 Allen, M. R. and Ingram, W. J.: Constraints on future changes in climate and the hydrologic cycle, *Nature* 419, 224-232,
261 2002.

262 Altaratz, O., Koren, I., Remer, L. A. and Hirsch, E.: Review: Cloud invigoration by aerosols -coupling between microphysics
263 and dynamics, *Atmos. Res.*, 140-141, 38-60, 2014.

264 Bollasina, M. A., Ming, Y., and Ramaswamy, V.: Anthropogenic aerosols and the weakening of the South Asian summer
265 monsoon, *Science* 334, 502-505, 2011.

266 Bond, T. C., and Coauthors: Bounding the role of black carbon in the climate system: A scientific assessment, *J. Geophys.*
267 *Res.*, 118, 5380-5552, 2013.

268 Bond, T. C., Zarzycki, C., Flanner, M. G., and Koch, D. M.: Quantifying immediate radiative forcing by black carbon and
269 organic matter with the Specific Forcing Pulse, *Atmos. Chem. Phys.* 11, 1505-1525, 2011.

270 Bosilovich, M. G., Schubert, S. and Walker, G.: Global changes of the water cycle intensity, *J. Climate* 18, 1591-1607,
271 2005.

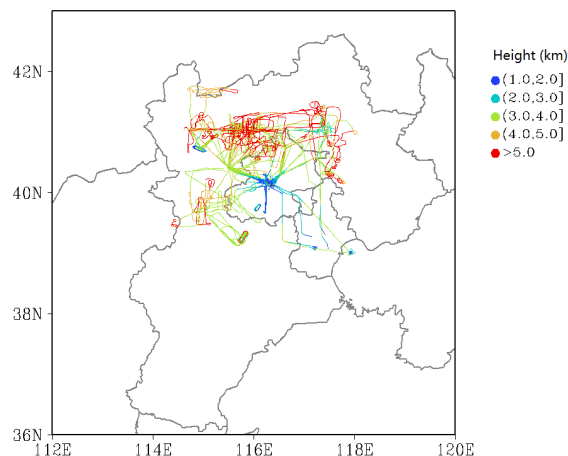
272 Choi, Y. S., Ho, C. H., Kim, J., Gong, D. Y. and Park, R. J.: The impact of aerosols on the summer rainfall frequency in
273 China, *J. Appl. Meteor Climatol.* 47, 1802-1813, 2008.



- 274 Fan, J., Leung, L. R., Rosenfeld, D., Chen, Q., Li, Z., Zhang J. and Yan H.: Microphysical effects determine macrophysical
275 response for aerosol impacts on deep convective clouds. *Proc. Natl. Acad. Sci.* 110, E4581-E4590, 2013.
- 276 Fan, J., Rosenfeld, D., Yang, Y., Zhao, C., Leung, L. R. and Li, Z.: Substantial contribution of anthropogenic air pollution to
277 catastrophic floods in southwest China, *Geophys. Res. Lett.* 42, 6066-6075, 2015.
- 278 Fu, Q., Johanson, C. M., Wallace, J. M. and Reichler, T.: Enhanced midlatitude tropospheric warming in satellite
279 measurements, *Science* 312, 1179, 2006.
- 280 Grant, L. D. and van den Heever, S. C.: Microphysical and dynamical characteristics of low-precipitation and classic
281 supercells, *J. Atmos. Sci.* 71, 2604–2624, 2014.
- 282 Guo X. L., Fu, D. H., Guo, X. and Zhang, C. M.: A case study of aerosol impacts on summer convective clouds and
283 precipitation over northern China, *Atmos. Res.* 142, 142-157, <http://dx.doi.org/10.1016/j.atmosres.2013.10.006>, 2014.
- 284 IPCC, In Summary for Policymakers, in *Climate Change 2007: The Physical Science Basis*, Contribution of Working Group
285 I to the Fourth Assessment Report of the Intergovernmental Panel on Climate Change. Cambridge: Cambridge University
286 Press, 1-18, 2007.
- 287 Khain, A. P., Rosenfeld, D. and Pokrovsky, A.: Aerosol impact on the dynamics and microphysics of deep convective clouds,
288 *Quart. J. Roy. Meteor. Soc.* 131, 2639-2663, 2005.
- 289 Koren, I., Martins, J. V., Remer, L. A. and Afargan, H.: Smoke invigoration versus inhibition of clouds over the Amazon,
290 *Science* 321, 946-949, 2008.
- 291 Kumar, A., Yang, F., Goddard, L. and Schubert, S.: Differing trends in the tropical surface temperatures and precipitation
292 over land and oceans, *Journal of Climate*, 17, 3, 653-664, 2004.
- 293 Lau, K. M. and Wu, H. T.: Detecting trends in tropical rainfall characteristics, 1979-2003, *Int. J. Climatol.*, 27, 979-988,
294 2007.
- 295 Levin, Z. and Cotton, W. R.: *Aerosol pollution impact on precipitation: A scientific review*, Springer, 386, 2009.
- 296 Li, Z., Niu, F., Fan, J., Liu, Y., Rosenfeld, D. and Ding, Y.: Long-term impacts of aerosols on the vertical development of
297 clouds and precipitation, *Nat. Geosci.* 4, 888–894, 2011.
- 298 Liu, S. C., Fu, C., Shiu, C. J., Chen, J. P. and Wu, F.: Temperature dependence of global precipitation extremes, *Geophys.*
299 *Res. Lett.* 36, L17702, doi: 10.1029/2009GL040218, 2009.
- 300 New, M., Todd, M., Hulme, M. and Jones, P.: Precipitation measurements and trends in the twentieth century, *J. Climatol.*
301 21, 1899–1922, 2001.
- 302 Qian, W., Fu, J., and Yan, Z.: Decrease of light rain events in summer associated with a warming environment in China
303 during 1961-2005, *Geophys. Res. Lett.* 34, L11705. DOI: 10.1029/2007GL029631, 2007.
- 304 Qian, Y., Gong, D. Y., Fan, J. W., Leung, L. R., Bennartz, R., Cheng, D. L. and Wang, W. G.: Heavy pollution suppresses

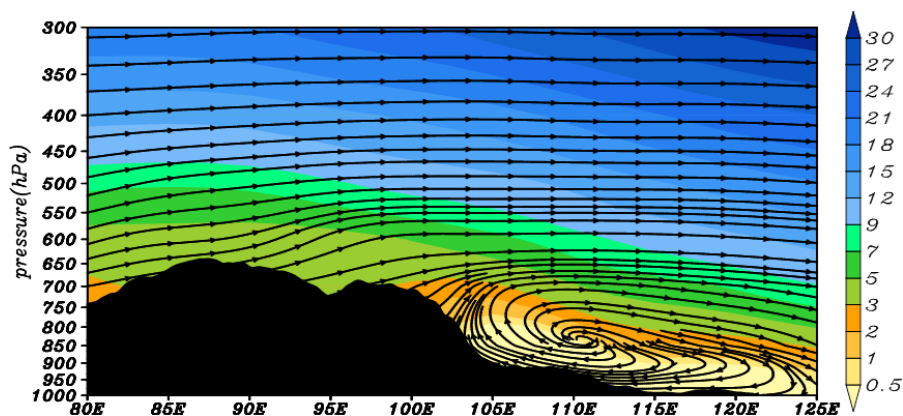


- 305 light rain in China: Observations and modeling, *J. Geophys. Res.*, 114, D00K02, doi: 10. 1029/2008JD011575, 2009.
- 306 Ramanathan, V., Chung, V. C. and Kim, D.: Atmospheric brown clouds: Impacts on South Asian climate and hydrological
307 cycle, *Proc. Natl. Acad. Sci.* 102, 5326–5333, 2005.
- 308 Ramanathan, V., Ramana, M. V. and Roberts, G.: Warming trends in Asia amplified by brown cloud solar absorption,
309 *Nature* 448, 575–578, 2007.
- 310 Rosenfeld, D. and Coauthors.: Flood or drought: How do aerosols affect precipitation? *Science* 321, 1309–1313, 2008.
- 311 Rosenfeld, D., Dai, J., Yu, X., Yao, Z., Xu, X., Yang, X. and Du, C.: Inverse relations between amounts of air pollution and
312 orographic precipitation, *Science* 315, 1396–1398, 2007.
- 313 Seinfeld, J.: Atmospheric science: Black carbon and brown clouds, *Nat Geosci* 1, 15–16, 2008.
- 314 Stevens, B. and Feingold, G.: Untangling aerosol effects on clouds and precipitation in a buffered system, *Nature* 461,
315 607–613, 2009.
- 316 Tao, W. K., Li, X., Khain, A., Matsui, T., Lang, S. and Simpson, J.: Role of atmospheric aerosol concentration on deep
317 convective precipitation: Cloud-resolving model simulations, *J. Geophys. Res.*, 112, D24S18, 2007.
- 318 Trenberth, K. E., Dai, A., Pasmussen, R. M. and Parsons, D. B.: The changing character of precipitation, *Bull. Am. Meteorol.*
319 *Soc.* 84, 1205–1217, 2003.
- 320 Van den Heever, S. C., Carrió, G. G., Cotton, W. R., DeMott, P. J. and Prenni, A. J.: Impact of nucleating aerosol on Florida
321 storms. Part I: Mesoscale simulations, *J. Atmos. Sci.* 63, 1752–1775, 2006.
- 322 Wang, Y. and Zhou, L.: Observed trends in extreme precipitation events in China during 1961–2001 and the associated
323 changes in large-scale circulation, *Geophys. Res. Lett.* 23, L09707, doi:10.292005GL022574, 2005.
- 324 Zhai, P.M., Ren, F. M. and Zhang, Q.: Detection of trends in China's precipitation extremes, *Acta Meteorologica Sinica*, 57,
325 208–215, 1999.
- 326 Zhang, H., Wang, Z. L., Guo, P. W., and Wang, Z. Z.: A modeling study of the effects of direct radiative forcing due to
327 carbonaceous aerosol on the climate in East Asia, *Adv. Atmos. Sci.*, 26, 57–66, 2009.
- 328

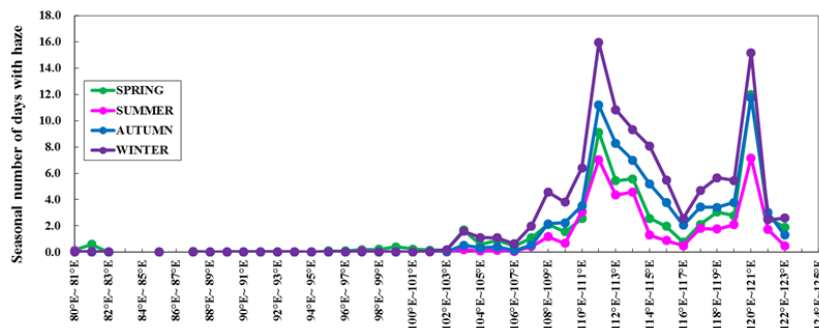


329

330 **Figure 1** Area and tracks of 40 aircraft flights carried out in Beijing and its surrounding regions during aerosol-cloud experiment
 331 from 2008 to 2010 by the Beijing Weather Modification Office

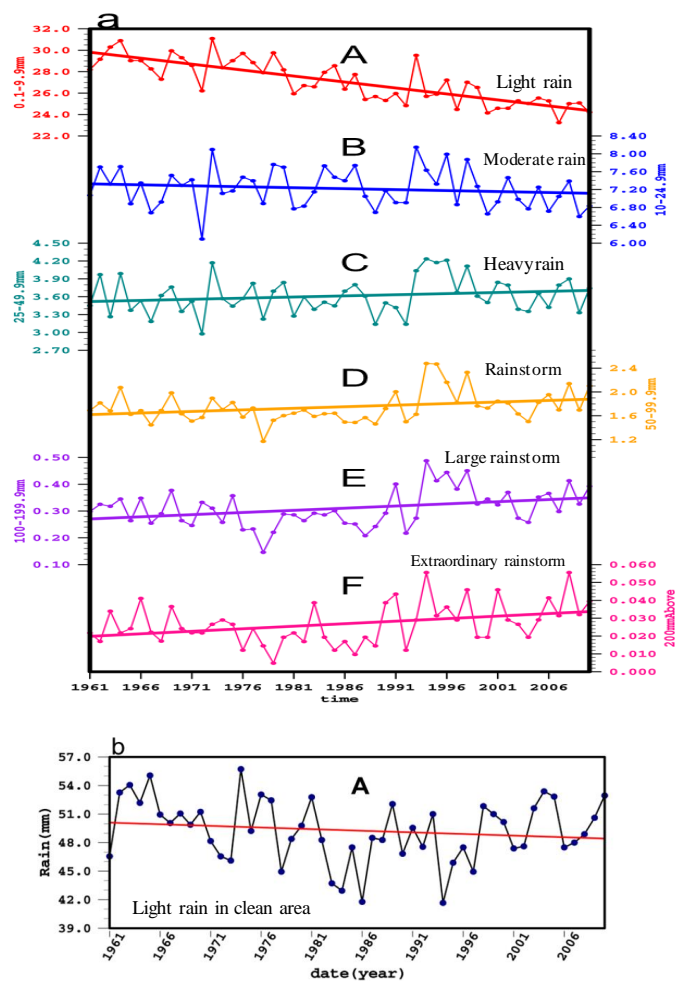


332

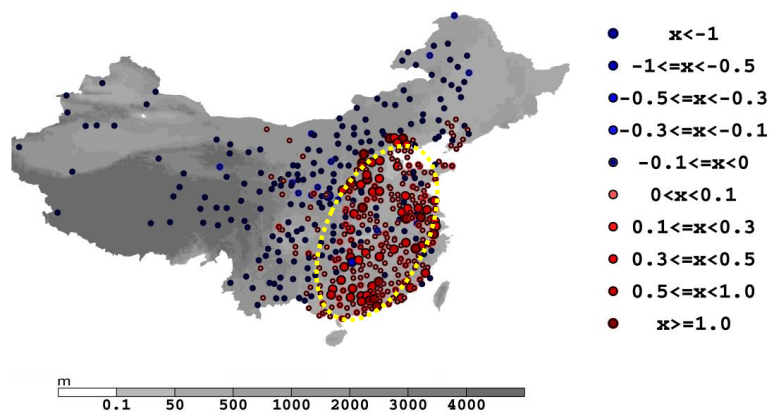


333

334 **Figure 2.** Cross sections of vertical circulations illustrated by stream lines (upper panel) with the horizontal wind speed (m s^{-1} ;
 335 color contours) and zonal variations of annual haze event frequency (lower panel) at 27°N - 41°N averaged in spring, summer,
 336 autumn and winter over 1961-2012. Note that near-surface vertical and horizontal winds are not illustrated well here due to
 337 north-south variations in the terrain and approximation of the location of the plateaus (black shaded area) in upper panel. All
 338 fields are for the annual-averages.



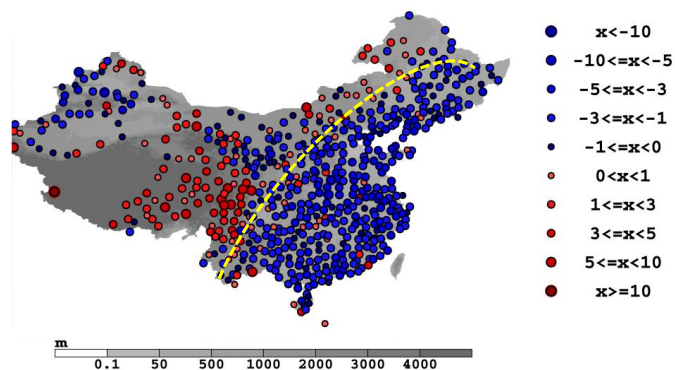
339 Figure 3 Interannual variation trends in (a) various precipitation intensities in the high aerosol concentration area in eastern
 340 China (east of 110° E) and (b) light rain in relative clean area of Qinghai Tibet Plateau; Note: Various precipitation intensities
 341 included light rain (A), moderate rain (B), heavy rain (C), rainstorm (D), large rainstorm (E), and extraordinary storm (F).



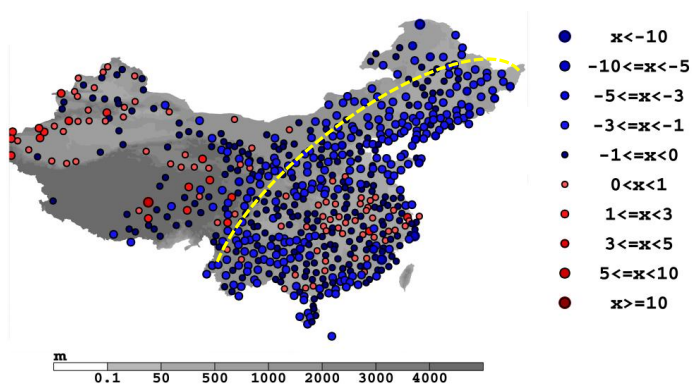
342



343

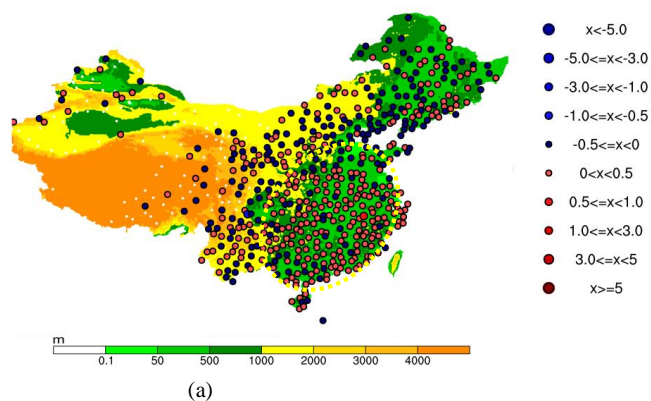


344



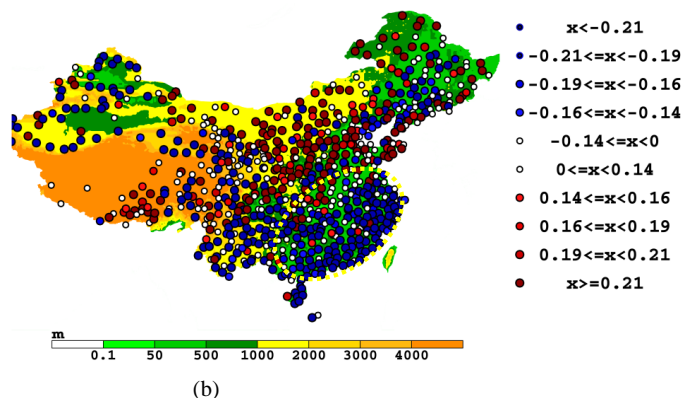
345 **Figure 4** Interannual variability distribution of haze frequency (a), visibility (b) and light rain frequency (c) in summer in
 346 mainland China in 1961-2010.

347



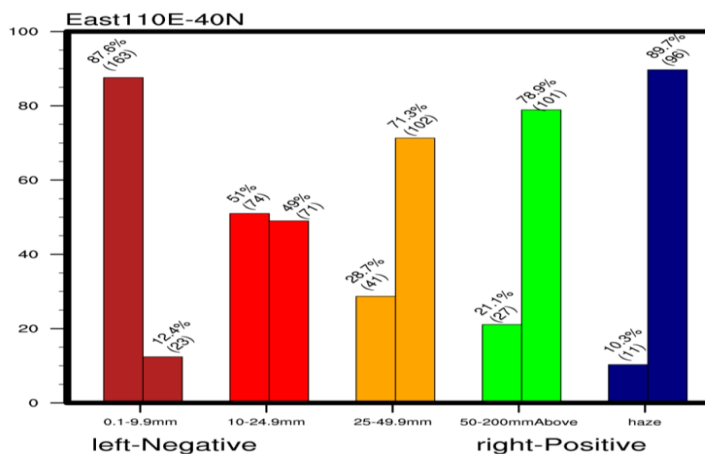
348

349

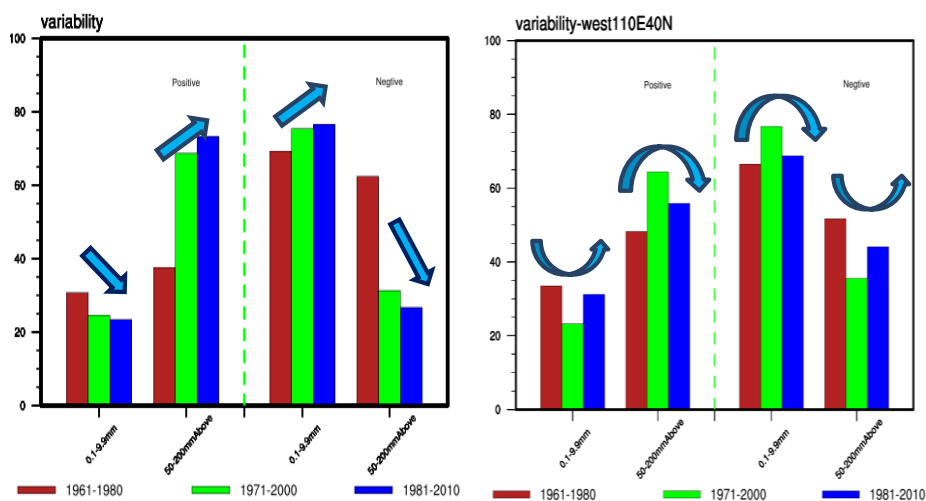


350
 351
 352
 353

Figure 5 The spatial distributions of (a) trends in summertime rainstorm frequency over 1961-2010 in China and (b) correlation coefficients between visibility and low cloud amount in summer of 1961-2010.



354



355

356

357

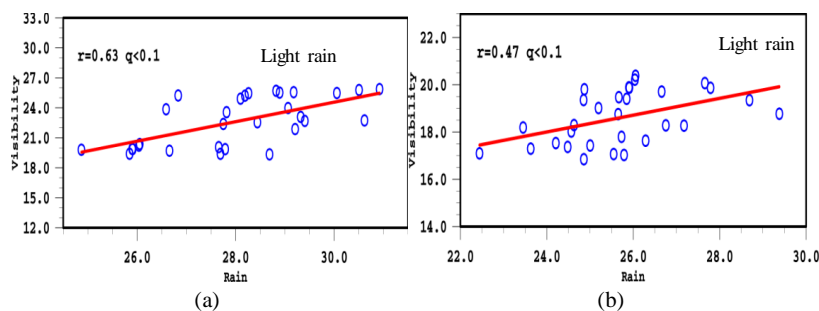
358

Figure 6 The ratio of summer haze days and the stations covered by positive and negative variability at various precipitation grades from 1961 to 2010 over in east of 110 E, south of 40 N (a), west of 110 E, south of 40 N (b). 601 precipitation stations and 598 visibility stations in eastern China. The right side is the positive variability and left side is the negative variability)

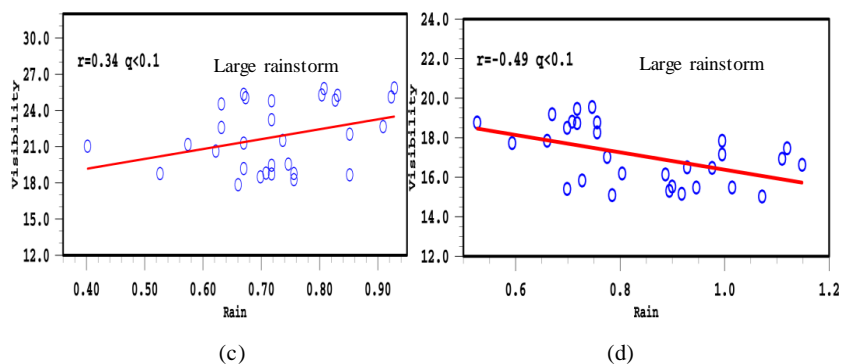
359



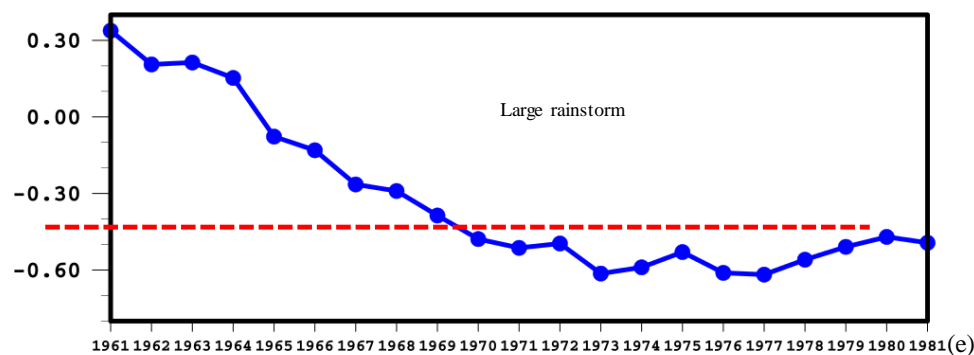
360
 361



362
 363

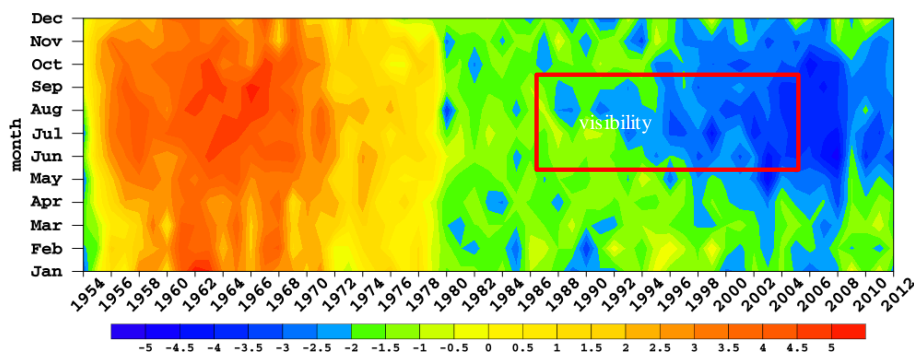


364

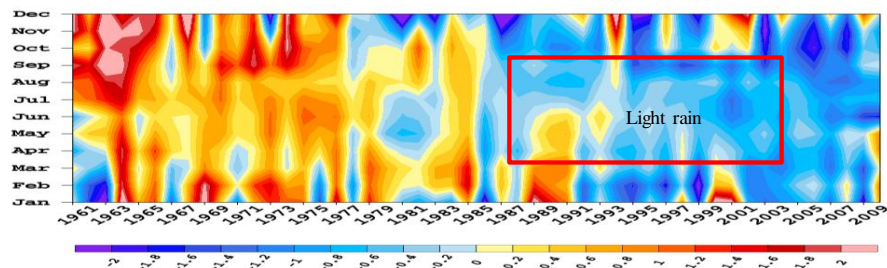


365 Figure 7 Correlation between summer average visibility (June, July and August) and light rain frequency in 1961-1990 (a), light
 366 rain frequency in 1981-2010 (b), extremely heavy rain event frequency in 1961-1990 (c), extreme heavy rain event frequency in
 367 1981-2010 (d) and the 20-year running correlation coefficients of visibility and precipitation (e), over eastern China (east to 110 °E,
 368 south to 40 °N)

369
 370

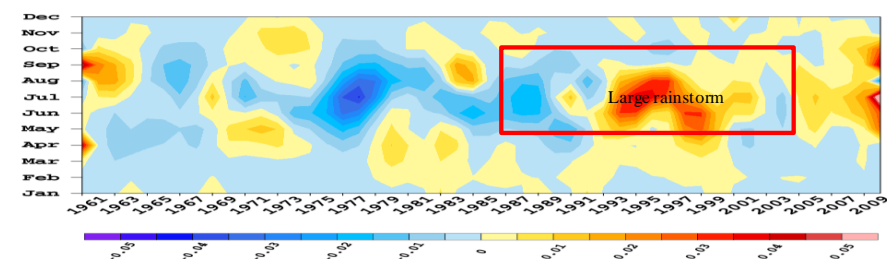


(a)



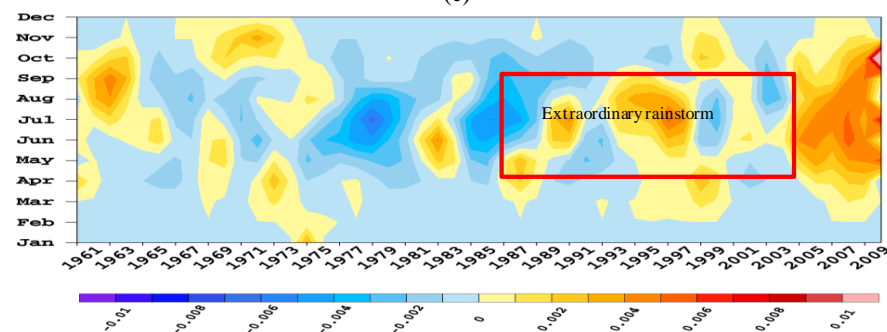
371
 372

(b)



373
 374

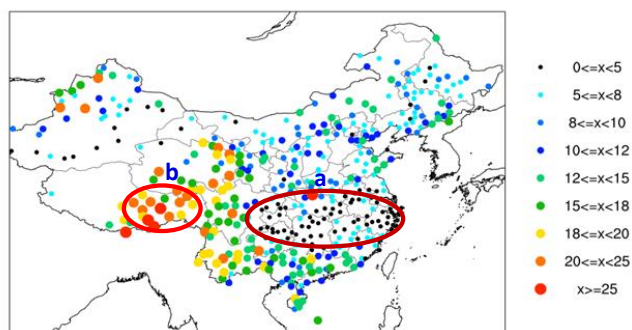
(c)



375
 376
 377
 378
 379

(d)

Figure 8 Annual cross-section of monthly anomaly of visibility (a), light rain (b), heavy rain (c), and extremely heavy rain (d)

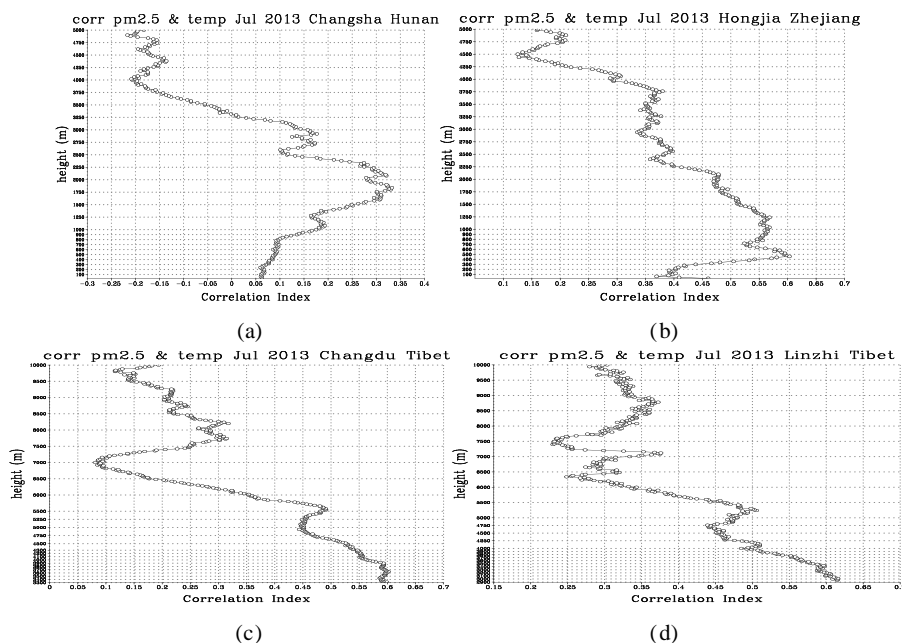


380
 381
 382
 383

Figure 9 Light rain frequency distribution of 601 stations in China in July of 2013. The circled region on right is the low-frequency light rain region in middle and downstream region of Yangtze River in eastern China, and that on left is the high-frequency light rain region in relative clean region over Tibet plateau.

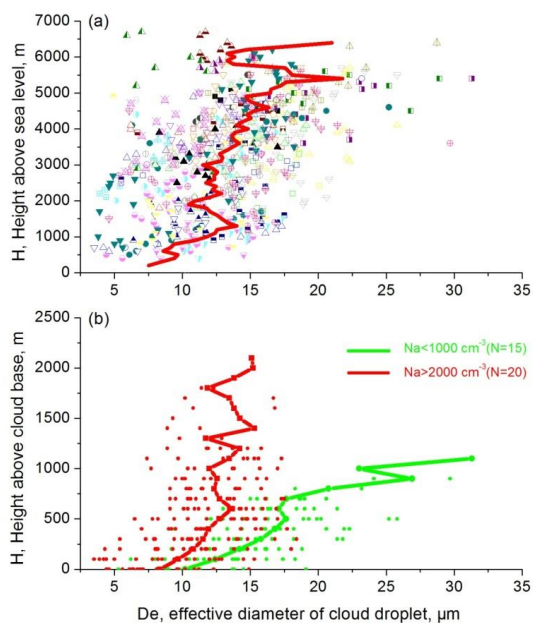


384
 385



386
 387
 388
 389
 390
 391

Figure 10 Correlation coefficient profiles between the daily $PM_{2.5}$ concentration (12 hour intervals) and atmospheric temperature at different vertical layer from L-band sounding for representing low-frequency light rain regions at stations of Changsha, Hunan (a) and Hongjia, Zhejiang (b), and for representing high-frequency light rain regions at relative "clean area" at stations of Linzhi (c) and Dingri (d) of Qinghai Tibet Plateau.



392
 393
 394

Figure 11 The vertical profiles of sampling cloud droplets data at each level under different aerosol state(a) and concentration(b) detected by 40 aircraft(Green profile: cloud droplets diameter under low concentration; Red profile: cloud droplets diameter



395 under high concentration).